BMC Musculoskeletal Disorders

RESEARCH

Open Access

Computer-navigated, stereotactic navigation for percutaneous radiofrequency ablation of osteoid osteomas: dose comparison and procedure times

Chiara Schmidli[1*], Frank Mosler[1], Danielle V. Bower[2], Gerd Nöldge[1], Johannes Heverhagen[1] and Nando Mertineit[1,3]

Abstract

Purpose Treatment of medication-refractory osteoid osteoma is typically performed with minimally-invasive percutaneous techniques, such as radiofrequency ablation. Given the typically young age of the population of patients being treated, we sought to assess whether using a 3D CT guidance system reduces the number of required probe repositionings and the number of required CTs to validate probe positioning in order to reduce the radiation dosage to the patient.

Methods We retrospectively reviewed the records of 19 patients who underwent procedures at our clinic amounting to a total of 27 ablations between 2012 and 2022. At the time of each procedure, the operating physician made the decision whether or not to use stereotactic navigation assistance. We analyzed the data using a Bayesian approach to elucidate possible differences between procedures conducted with or without navigation.

Results Our results showed a statistically and clinically-significant administration of, on average, 200 mGy*cm greater radiation dosage to the patient when stereotactic navigation was used to guide RFA probe placement for ablation of osteoid osteomas compared with not using navigation assistance. There was a trend towards requiring one fewer probe repositioning with navigation assistance, however this was not statistically conclusive. There was no difference in the time required to achieve the target probe placement or in total procedure duration whether stereotactic navigation was used or not.

Conclusion When utilizing a 3D-guided stereotactic navigation system, there is likely a learning phase before the potential benefits of such a system are realized. Additional radiation administration to the patient may result from the operator learning to properly use and trust the system. In our case, the data also likely reflect a bias in operator choice to use the navigation system when the lesions are more difficult to correctly target or multiple ablation positions are necessary, while choosing conventional imaging assistance for easily targetable tumors, which may conceal some of the benefit of using the navigation system.

Keywords Osteoid osteoma, Radiofrequency ablation, Guided navigation, Radiation dosage

*Correspondence:
Chiara Schmidli
chiara.giancamilli@outlook.com
Full list of author information is available at the end of the article

Background

Osteoid osteoma is a benign osteoblastic bone lesion of undetermined etiology, which was first described by Dr. Henry L. Jaffe in 1935 [1]. The incidence is 2–3% of primary bone tumors (the third most common benign bone tumor), or 10–1% of benign skeletal lesions [2–4]. 50% of patients are children, adolescents, and young adults aged 10–20 years, with a male-to-female ratio of 4:1 [5].

The classic clinical symptomatology of osteoid osteoma consists of progressively intensifying pain that is typically worse at night and responds well to non-steroidal anti-inflammatory drugs (NSAIDs). The pain is thought to result from prostaglandins produced by the tumor which cause local vasodilation and compress the abundant nerve endings in the tumors [6]. Prostaglandins also induce hyperalgesia, which intensifies the pain. Thus, the prostaglandin-suppressing effect of NSAIDs dramatically reduces the pain.

In most cases, the diaphysis or metaphysis of long bones of the lower extremity are affected, most commonly the femur or tibia. Less frequently affected bones are those of the hand or feet. In 10–20% of cases, osteoid osteoma manifests in the spine, typically causing painful scoliosis [7, 8]. The tumor is predominantly eccentrically cortically or subcortically localized, less commonly medullary (spongy) or subperiosteal.

Radiologically, osteoid osteoma is typically seen as a central nidus of less than 2 cm diameter with variable bone mineralization, which is surrounded by a zone of reactive sclerosis with cortical thickening and bone marrow edema [9]. On CT, the nidus appears as a small, well-defined, hypodense (lytic) area. Thin vascular fibrils surrounding the lesion are highly specific for distinguishing an osteoid osteoma from other radiolucent bone tumors on CT [5]. On MRI, the nidus generally presents with low to moderate signal intensity on T1-weighted images and variable intensity on T2-weighted images depending on the amount of mineralization [10]. Typically, there is extensive bone edema surrounding the nidus, which may extend a considerable distance through the affected bone. Following contrast administration, the nidus typically shows arterial phase enhancement with early partial washout, although other enhancement patterns are possible [11]. Figure 1 portrays example images of osteoid osteomas.

Treatment of osteoid osteoma is predominantly conservative by means of NSAIDs as the tumors can regress spontaneously [12, 13]. If long-term NSAID use is necessary or not tolerated and/or if symptoms are severely limiting, the tumor may be locally treated. Treatment of osteoid osteoma was originally performed by en bloc resection with a published success rate between

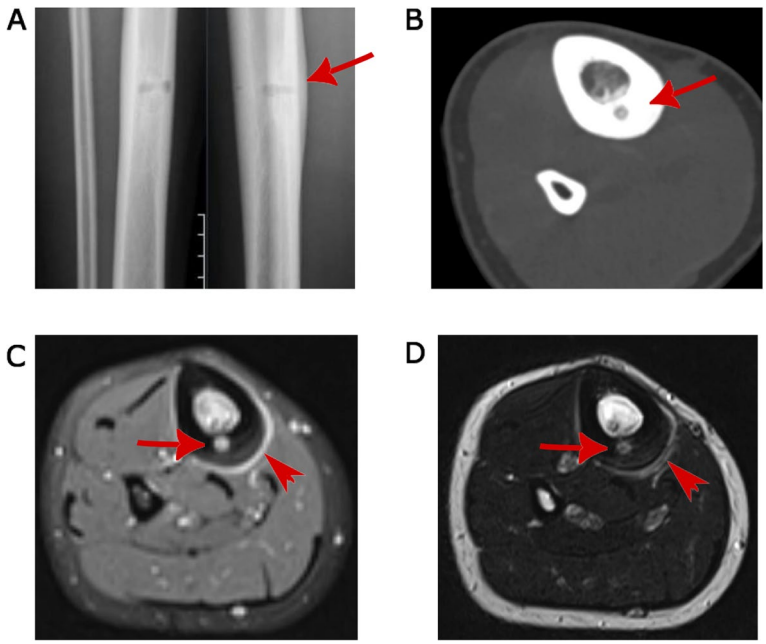

Fig. 1 Example images of osteoid osteoma. **A** The X-ray image shows the sclerotic bone thickening around the osteoid osteoma. **B** In the CT, the osteoid osteoma is seen as the central lucency with circumferential reactive bone sclerosis. **C** In the T1-weighted MRI image post-contrast, the tumor nidus is seen as hyperintensity within the thickened surrounding low intensity cortical bone (arrow). Hyperintense edema surrounds the reactive periostium (arrowhead). **D** The T2-weighted MRI image shows the mildly hyperintense tumor nidus (arrow) with periostial edema (arrowhead)

88%– 100% but recurrence rates of up to 25% [5]. Difficulty in locating the nidus intraoperatively can result in incomplete nidus removal and recurrence.

Therefore, less invasive percutaneous ablation under imaging guidance to successfully target the nidus has now replaced surgical resection as the gold standard [14]. Various percutaneous ablation techniques, including radiofrequency ablation (RFA), cryoablation, interstitial laser photocoagulation, and treatment with a combination of radiofrequency and alcohol ablation [15–19] have been established. Today, RFA is most commonly performed. Using percutaneous access, a radiofrequency antenna is inserted into the nidus to heat the tissue of the nidus to approximately 90 °C and destroy it. RFA was first described by Rosenthal et al in 1992 [20]. Since then, studies have reported equivalent or better results using RFA for the treatment of osteoid osteoma compared to surgical resection [4, 21, 22]. Recurrence rates following RFA are reported between about 5% and 20% [23–28]. Complications occur at a rate of 5% or less. Skin burns are the most commonly reported complication, while less common complications include muscle hematomas, infections, wound dehiscence, and nerve injuries [24, 29]. Compared with open surgical resection, however, percutaneous ablation presents the advantages of minimal scarring, low risk of injury to nearby structures, low post-operative bone fracture risk, and more rapid post-operative recovery [26, 28, 30].

Complete ablation of the tumor nidus is the most important factor for the successful treatment of osteoid osteoma [31]. To guide accurate access and probe placement for ablation, CT has become the most commonly utilized imaging method as it is easier to implement and more readily available than MRI. However, CT guidance carries the disadvantage of imparting ionizing radiation, which is an important concern given that the majority of patients being treated for osteoid osteoma are children and young adults. Reducing the number of required CT scans through accurate initial probe placement and minimizing remission and need for re-treatment are therefore important.

Successful treatment of osteoid osteoma with a reduction in administered radiation has been reported using 3D CT navigation, such as the O-arm with Stealth System navigation [32–34]. We sought to test whether the CAS-One IR navigation system (Casone IR, Cascination, Berne, Switzerland), which has been successfully used to guide liver tumor ablations [35, 36], would enable us to ablate osteoid osteomas with fewer probe placement adjustments and fewer control CTs in order to reduce radiation dosage.

Methods

Informed consent was obtained from all of the participants in the study. The responsible cantonal ethics commission approved the study to retrospectively compare the needle positioning accuracy, procedure times, and radiation dosage of ablations performed with or without CAS-OneIR navigation guidance at the Inselspital Bern. The study was conducted in accordance with the Declaration of Helsinki.

Data acquisition

19 patients who underwent procedures for a total of 27 ablations between 2012 and 2022 were identified from our clinical records. Patient gender and age at the time of the procedure were recorded. The procedures were reviewed to collect the following information: number of required needle repositionings to correctly place the RFA probe in the nidus, time (minutes) to successful probe placement, total procedure duration (minutes), total radiation dosage of the procedure (DLP, mGy*cm), radiation dosage per ablation. In three of the procedures performed with the navigation system, two sites were ablated during the procedure. For all other procedures, only one ablation was performed per procedure.

Surgical procedures

The surgical procedures were performed in the interventional radiology CT-suite at the Bern University Hospital, Inselspital, Bern, Switzerland. All ablation procedures were performed under either general or spinal anesthesia. In all cases RFA probes with an active tip length of 7 or 10 mm were used (Cool-Tip, Medtronic, Dublin, Ireland). During conventional ablation (without stereotactic navigation), patients were positioned on the CT table according to the anticipated access route. After local disinfection and sterile draping, local anesthesia was administered followed by placement of the bone drill. After crossing the cortical bone, a biopsy was first taken from the nidus and then the RFA probe was placed in the nidus. The position of the probe was controlled using CT fluoroscopy and/or spiral CT.

When stereotactic navigation was to be used, pre-operative planning MRI or CT images were loaded into the CAS-One IR software prior to the operation at operator choice to co-register to intraoperatively-acquired images to better detect the nidus. Patients were immobilized on a vacuum mattress and the navigation arm for probe placement was fixed to the table. The body area of the target was sterile draped and 6 markers were placed around the anticipated puncture site. A native planning CT scan was performed and sent to the planning software of the CAS-One IR. The sterile-covered touch-screen of the navigation system was positioned in front of the surgical team

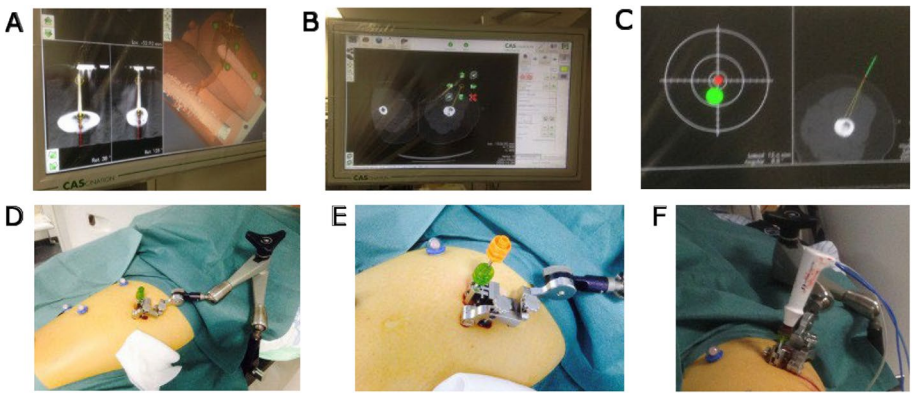

Fig. 2 Surgical setup. **A** After the surgeon marks identifiable landmarks, the software calibrates and displays the intended access route. **B** The interoperative images displayed on the stereotactic navigation screen portray the calculated access route for probe placement. **C** As the navigation arm guides probe placement, repeat images show the current position of the probe (red) relative to the target positioning (green). **D** The photo shows the mounting of the navigated arm on the operation table. **E** shows a closer view of the guidance sheaths positioned by the arm. **F** shows the navigated arm with RFA probe inserted to perform the ablation

within easy reach. Stereotactic placement of the probe was performed as previously published [37]. Briefly: the target visualized on the planning CT and the skin entry point were marked in the planning software. This enabled the navigation software to calculate and guide optimal instrument placement. The navigation arm was placed according to the software. Through the guiding tool, local anesthesia was administered, and bone access was established using a bone drill, depending on the operator choice. A biopsy was taken from the nidus and sent for pathological analysis.

Upon placement of the probe in the target nidus, a further CT or CT fluoroscopy was taken to verify correct probe placement. If found to be necessary, intermittent control CTs or CT fluoroscopy images were acquired. Figure 2 shows the interventional setup. Following verification of the correct RFA needle positioning in the tumor nidus, the ablation was performed with a target temperature of 90 °C using 7 mm or 10 mm Cool-Tip RFA probes (Medtronic, Dublin, Ireland) for up to 5–10 minutes, according to the interventionalist's assessment.

Statistical analyses

Our objective was to assay potential differences between procedures performed with and without stereotactic navigation for four metrics: the required number of probe repositionings, time to target, total procedure time, and radiation dosage. This objective naturally lent itself to performing a Bayesian parameter estimation [38], which is also more reliable with small datasets. It was assumed that the data are described by a Student's t-distribution, which gives rise to the estimation of 5 parameters for each metric: the mean and standard deviation with and without navigation, as well as a normality parameter that captures the influence of outliers. Using the posterior distributions of the parameters then permits the computation of distributions that show the differences between the parameters with and without stereotactic navigation. To interpret these differences we imposed additional criteria that defined a range over which the differences, albeit statistically relevant, would not generally be regarded as clinically relevant. In short, Bayesian inference provides a robust estimate of differences between groups and, importantly, inherently includes uncertainty in claiming whether two groups are different [39, 40].

A Bayesian model requires the specification of a prior for each parameter, which captures prior knowledge of the range of values that a parameter may take. For the priors, we chose broad and noncommittal distributions. For each metric the data were pooled to determine the pooled mean and pooled standard deviation (pooled std) which were used to construct the priors for the means with and without stereotactic navigation. The prior distributions for the standard deviations were uniform for each metric and were the same for the parameters with and without stereotactic navigation:

- Number of repositionings: 1/1000th to 10x the pooled std.
- Time to target placement: 1/100th to 100x the pooled std.
- Total procedure duration: 1x to 50x the pooled std.
- Total radiation dosage: 1x to 500x the pooled std.

The prior distribution for the normality parameter was $\frac{1}{\lambda}e^{\frac{-(\nu-1)}{\lambda}}$ where, $\lambda = 29$ accommodates normally and non-normally distributed data. This completed the

specification of the priors on the parameters we estimated from our Bayesian model.

The final step to enable interpretation of the posterior parameter distributions was to define a so-called 'region of practical equivalence (ROPE)'. This was defined based on domain expertise and an understanding of how the results should be interpreted in the clinical context. Importantly, ROPEs are defined completely independently from the Bayesian parameter estimation. Data that fall within the bounds of a ROPE should be considered as having the same interpretation or relevance given a particular clinical context, i.e. differences that fall within the bounds of the ROPE are clinically insignificant. The ROPE for each metric was set as follows: a difference of 20 minutes for time (− 20 to 20), a difference of 1 for probe repositioning (− 1 to 1), and a difference of 50 mGy*cm for radiation dose (− 50 to 50). The interpretation is that a difference of less than 20 minutes in procedure time or less than 50 mGy*cm (equating to 2 or 3 X-rays) is insignificant practically speaking [41], but a difference of one single replacement of the probe is significant. The effect size conveys a measure of how distinctly separated two groups are, or how much the variability within each group could explain the difference of the means. An effect size of less than − 0.1 or greater than 0.1 is broadly considered a meaningful difference.

Results

From the selected procedures where an ablation of one or more osteoid osteomas was performed, metrics on each procedure were retrospectively reviewed, including:

1) the number of required needle repositionings to correctly place the RFA probe in the tumor nidus,
2) time (minutes) to target probe placement,
3) total procedure duration (minutes),
4) total radiation dosage of the procedure (DLP, mGy*cm) and the radiation dosage per ablation.

Only three procedures involved ablation of two tumors, and the remainder involved only a single ablation. The total radiation dosage of the procedure and dosage per ablation provided similar results, therefore we present the data for total radiation dosage of the procedure, which is clinically more important than the dosage per tumor ablation, and summarize the data per ablation.

Table 1 summarizes the age and sex of the patients and location of the tumors that were ablated with or without stereotactic navigation.

These retrospectively assembled metrics were then analyzed using Bayesian estimation to assess the evidence for differences between procedures performed using stereotactic navigation and procedures performed without navigation assistance. For each parameter and each treatment group (with or without stereotactic navigation), the plausible distributions of mean values consistent with the data were modelled. This is far more representative of the true underlying population of data from which the samples are drawn, particularly for a small number of samples, as opposed to calculating the mean of the selected samples and assuming that it accurately represents the true mean of the broader underlying population of possible outcomes.

Table 1 Comparison of ablated tumors in each treatment group

	With stereotactic navigation	Without stereotactic navigation
Total number of ablations	**16**	**9**
Sex of patient		
Female	7	4
Male	9	5
Average age (age range), years	23 (6—47)	25 (15—48)
Tumor location		
Tibia	4	4
Fibula	3	1
Femur	6	2
Humerus	2	2
Talus	1	0

Each data figure displays the data for one metric and depicts the plausible distribution of means for the given metric for procedures performed with stereotactic navigation (subplot A) or without (subplot B). The difference of means subplot in each figure shows the distribution of the pairwise differences of these sampled means for each iteration of the model. The 95% high density interval (95% HDI, black line) shows where 95% of the credible values for the given parameter lie. The region of practical equivalence (ROPE, green line) is subjectively defined and specific to the individual metric as defined in the Methods. Values which lie within this ROPE range are considered to be clinically equivalent. Including a ROPE in the analysis conveys if a statistical difference between groups is a clinically relevant difference or not. When approximately 5% or less of the 95% HDI overlaps with the ROPE, the difference between groups is generally speaking considered to clinically relevant.

Trend towards fewer probe repositionings required when using stereotactic navigation

The plausible mean number of probe repositionings required to reach the target using stereotactic navigation is tightly centered around 0.0 (Fig. 3A) with an average standard deviation of 0.0 (Fig. 3E), while the plausible

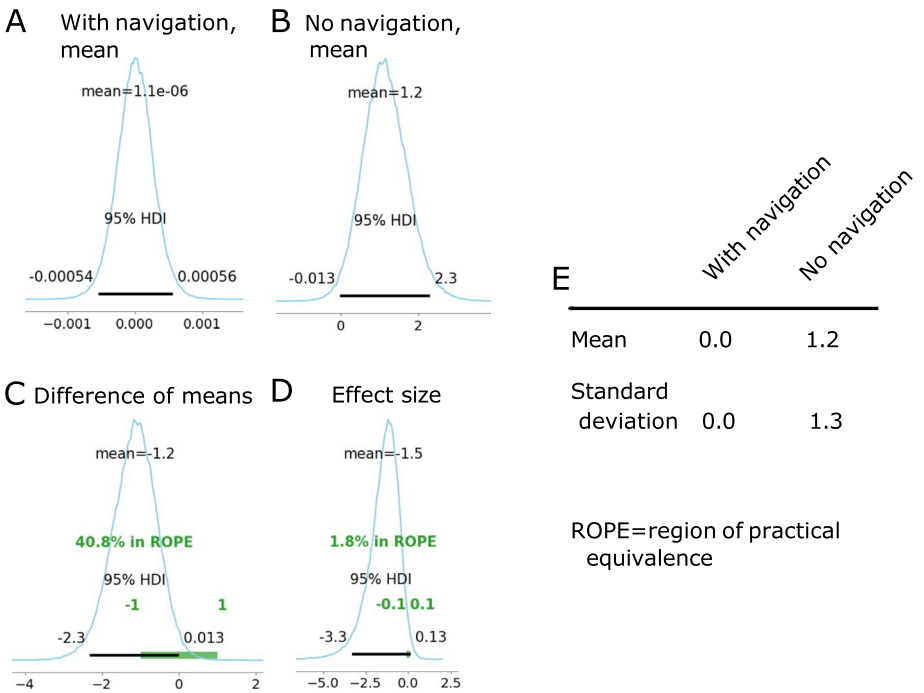

Fig. 3 No significant difference in required number of probe repositionings when using stereotactic navigation versus without navigation. The plausible distributions of mean values consistent with the data are shown for the number of required probe repositionings **A** with stereotactic navigation and **B** without navigation assistance. **C** shows the pairwise differences of these sampled means and **D** indicates a strength of the effect accounting for the amount of variability within the groups. **E** summarizes the average values of the mean and standard deviation distributions consistent with the data. In plots **A** through **D**, the black bars show where 95% of the credible values lie (95% HDI). The green bars in **C** and **D** show the region of practical (clinical) equivalence (ROPE). In **C**, the 95% HDI fractionally includes zero and more than 40% of the 95% HDI overlaps with the ROPE, meaning there is no difference in number of repositionings with or without navigation. However, the effect size in **D** is strong and only fractionally includes zero, suggesting a trend towards fewer repositionings using stereotactic navigation

mean number of repositionings required without stereotactic navigation is centered at 1.2 (Fig. 3B) with an average standard deviation of 1.3 (Fig. 3E). 95% of the credible differences of means between the treatment groups (Fig. 3C) lie between − 2.3 and 0.013. This range fractionally includes zero, which means a difference between the groups cannot be concluded. Similarly, 40.8% of the 95% high density interval (HDI) lies within the ROPE when one single repositioning was considered clinically relevant, which supports that there is no clinically relevant difference in number of repositionings when using stereotactic navigation versus without navigation. However, the difference in means between the treatment groups centers at 1.2 fewer repositionings required when stereotactic navigation is used (Fig. 3C), and the magnitude of the measured effect (effect size) is clinically significant: the 95% HDI for effect size fractionally includes zero, but the effect size of − 1.5 is a meaningful difference, and only 1.8% of the HDI falls within the ROPE (Fig. 3D). This suggests a trend towards requiring fewer repositionings when stereotactic navigation is used, but the difference is not conclusive with the small number of cases tested.

No difference in time required to place the probe in the target whether using or not using navigation

The plausible mean time to target probe placement is centered at 49 min when using stereotactic navigation (Fig. 4A), and 53 min without navigation (Fig. 4B). The distributions of standard deviations are comparable for the two groups, averaging 27 min with navigation and 25 min without navigation (summarized in Fig. 4E). The difference of means is centered very close to zero at − 3.8 min, with 90.1% of the plausible differences between the groups falling within the ROPE (Fig. 4C). Similarly, the effect size is centered approximately at zero (Fig. 4D). Therefore, the evidence indicates no difference in time to target probe placement when using stereotactic navigation compared to not using navigation.

No difference in total procedure time whether using or not using navigation

The distribution of the total procedure duration is centered at 69 min when using stereotactic navigation (Fig. 5A) and 68 min without navigation (Fig. 5B). These distributions have similar standard deviation distributions averaging 23 min with navigation and 22 min

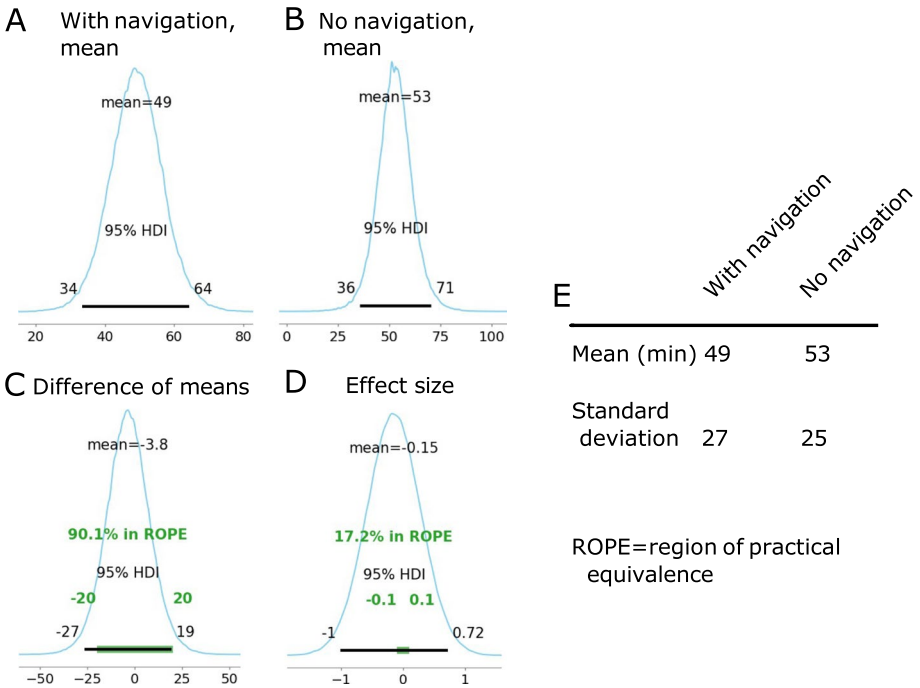

Fig. 4 No difference in time to target probe placement when using stereotactic navigation versus no navigation. The plausible distributions of mean values consistent with the data are shown for the time required for target probe placement **A** with stereotactic navigation and **B** without navigation assistance. **C** shows the pairwise differences of these sampled means and **D** indicates a strength of the effect accounting for the amount of variability within the groups. **E** summarizes the average values of the mean and standard deviation distributions consistent with the data. The mean time to target placement is very similar for both groups: **A** 49 min with stereotactic navigation and **B** 53 min without navigation with nearly equivalent standard deviations **E**. **C** The difference of means centers close to zero with 90.1% of the 95% HDI within the ROPE, indicating no difference in time to target probe positioning. **D** The effect size also centers at approximately zero and completely overlaps the ROPE, supporting no difference in time to target probe placement

without navigation, as summarized in Fig. 5E. The difference of means is centered very close to zero, at 0.82 with 94.7% of the 95% HDI for plausible differences in time falling within the ROPE (Fig. 5C). Likewise, the effect size is centered nearly at zero (0.039) and extends beyond both ends of the ROPE (Fig. 5D). These provide conclusive evidence for no difference in total procedure duration when using stereotactic navigation compared to no navigation.

The total radiation dosage is higher using stereotactic navigation

The plausible mean radiation dosage for the ablation procedure is centered at 428 mGy*cm when using stereotactic navigation (Fig. 6A) and 230 mGy*cm without navigation (Fig. 6B). There is much greater variability in the standard deviations using stereotactic navigation, with an average standard deviation of 266 mGy*cm (Fig. 6C) versus an average standard deviation of 120 mGy*cm without navigation (Fig. 6D). The difference in means between the treatment groups was highly significant, with a mean difference of 198 mGy*cm greater radiation dosage when using stereotactic navigation than without navigation, and the 95% HDI spans from 22 to 378, which importantly does not include zero (Fig. 6E). It can therefore be concluded that the total radiation dosage is higher with stereotactic navigation than without navigation in our patient sample. Furthermore, only 4.4% of the 95% HDI for the difference of means falls within the ROPE when a difference of 50 mGy*cm is considered clinically insignificant (Fig. 6E). This is strong evidence for a clinically relevant increase in radiation dosage when using stereotactic navigation versus without navigation in our clinical sample. Likewise, the magnitude of the effect (effect size) is highly significant with the 95% HDI ranging from 0.071 to 2, which excludes zero, and only 1.7% of the HDI falling within the ROPE (Fig. 6F).

Figure 6G summarizes the average values of the mean and standard deviations in total procedural radiation dosage and the clinically relevant increased radiation dosage per procedure using stereotactic navigation: the 95% HDI for the difference of means and effect size show minimal overlap with the ROPE. Additionally, Fig. 6G summarizes the differences in radiation dosage per ablation when using stereotactic navigation or without navigation. The dosage per ablation is slightly different than

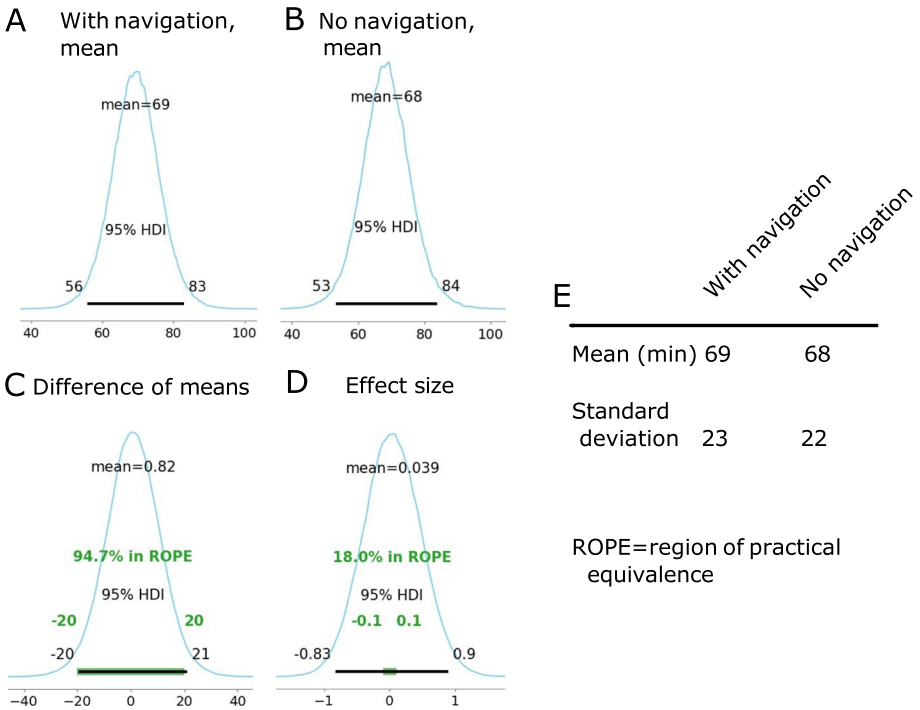

Fig. 5 No difference in total procedure time when using stereotactic navigation versus no navigation. The plausible distributions of mean values consistent with the data are shown for the total procedure time **A** with stereotactic navigation and **B** without navigation assistance. **C** shows the pairwise differences of these sampled means and **D** indicates a strength of the effect accounting for the amount of variability within the groups. **E** summarizes the average values of the mean and standard deviation distributions consistent with the data. The mean procedure time is nearly identical for both groups: **A** 69 min with stereotactic navigation and **B** 68 min without navigation. The average standard deviations are also nearly identical **E**. **C** The difference of means centers at approximately zero with 94.7% of the 95% HDI within the ROPE, indicating no difference in total procedure time. **D** The effect size also centers effectively at zero and completely overlaps the ROPE, supporting no difference in total procedure time when using stereotactic navigation or not

the overall radiation dosage per procedure because three patients treated using stereotactic navigation each had two tumors ablated within a single procedure. The evidence for increased radiation dosage using stereotactic navigation compared to without navigation was nearly as strong on a per-ablation basis as per procedure: only 7.2% of the 95% HDI for the difference of means falls within the ROPE and 2.4% for effect size (Fig. 6G).

Table 2 summarizes the mean and standard deviation values from Figures 3 - 6 for tumors ablated with or without stereotactic navigation.

Discussion

Our results indicate that using stereotactic navigation to guide RFA probe placement for ablation of osteoid osteomas involves a statistically and clinically-significant administration of, on average, approximately 200 mGy*cm greater radiation dosage to the patient compared with not using navigation assistance. The evidence do not conclude that fewer repositionings of the probe are required to achieve target probe placement using stereotactic navigation compared to without navigation assistance. However, the data show a strong trend towards one fewer repositioning required when using stereotactic navigation as the difference was nearly significant. The evidence conclusively demonstrated no difference in time to target probe placement and no difference in total procedure duration whether stereotactic navigation was used or not.

We employed Bayesian estimation as a more complete and robust approach to interrogate possible differences between ablation procedures conducted with or without stereotactic navigation. Bayesian inference evaluates the range of possible means and standard deviations of each metric which are consistent with the sampled data and fall within a credible range, rather than assuming that the sampled data perfectly represent the underlying populations from which those samples were drawn. This is especially important for small sample sizes, where the specific samples drawn could provide a grossly inaccurate representation of the true underlying population of data. Furthermore, Bayesian inference accommodates data from non-normal distributions, including outliers.

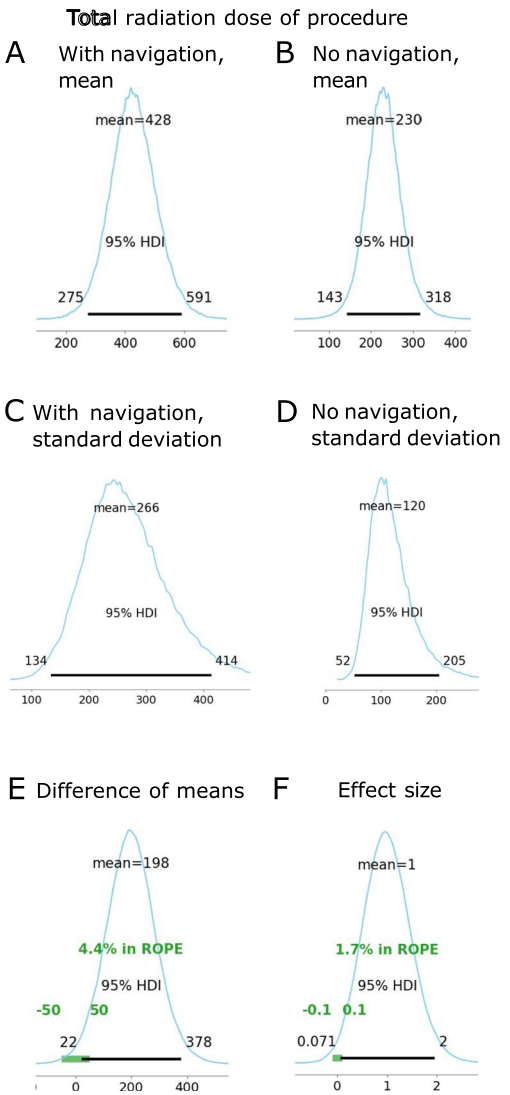

G

	With navigation	No navigation
Per Ablation		
Mean dose (mGy*cm)	389	231
Standard deviation	216	123
Difference of means	7.2% in ROPE	
Effect size	2.4% in ROPE	
Entire Procedure		
Mean dose (mGy*cm)	428	230
Standard deviation	266	120
Difference of means	4.4% in ROPE	
Effect size	1.7% in ROPE	

ROPE=region of practical equivalence

Fig. 6 Total administered radiation dosage is higher when using stereotactic navigation than without navigation. The plausible distributions of mean values consistent with the data are shown for the average total radiation dosage **A** 428 mGy*cm with stereotactic navigation and **B** 230 mGy*cm without navigation assistance. There is also greater variability in administered radiation dosage with a wider distribution of the standard deviation with stereotactic navigation seen in **C** versus without navigation as seen in **D**. **E** shows the pairwise differences of these sampled means with statistically significantly more radiation delivered when using stereotactic navigation. The 95% HDI excludes zero and only 4.4% of the HDI lies within the ROPE. **F** The strong effect size also excludes zero with only 1.7% of the 95% HDI within the ROPE, indicating the significant difference between the groups. **G** summarizes the average values of the mean, standard deviation, difference of means, and effect size for the radiation dosage of the entire procedure as well as per ablation. The data per ablation differ slightly because three patients had two tumors which were ablated within the same procedure

Nevertheless, these results must be considered in the context of limitations of the study. The data upon which the statistical analyses are based were retrospectively collected by review of clinical records, which in itself is subject to error in the accuracy of the assembled data. The amount of error in the raw data values is unknown. For instance, while the timestamps on CT images and radiation are objective, there is no documentation of, for instance, interruptions to the procedure due to an urgent phone call or other disruption, which would contribute to the reported time duration even though the time was not being utilized to conduct the steps of the procedure.

Similarly, the radiation output is an objective measure, but the length of the CT region performed is subjectively determined. Different operators likely have different preferences on how large of a region around a tumor to image, and the anatomical location of the tumor and adjacent structures will also influence the scan volume.

Table 2 Summary of mean and standard deviation values for all metrics

	With navigation	Without navigation
Number of probe repositionings (Fig. 3)		
Mean	0.0	1.2
Standard deviation	0.0	1.3
Time to target probe placement (Fig. 4)		
Mean (min)	49	53
Standard deviation	27	25
Total procedure time (Fig. 5)		
Mean (min)	69	68
Standard deviation	23	22
Total radiation dosage of the procedure (Fig. 6)		
Mean (mGy*cm)	428	230
Standard deviation	266	120
Difference of means: 4.4% in ROPE		
Effect size: 1.7% in ROPE		

These factors affect the total radiation dosage administered regardless of whether stereotactic navigation assistance is used for a procedure or not.

Additionally, there are important confounding factors which must be considered in interpreting the results of this study. Firstly, there was no randomization to determine whether a procedure would be conducted with or without stereotactic navigation. Each operator decided personally whether or not to use navigation assistance. This introduces a considerable bias, whereby operators were more likely decide to use stereotactic navigation when the position of the tumor with respect to adjacent anatomical structures was more difficult to access or where there was a higher risk of piercing sensitive tissues in close vicinity. If the procedures had been randomly assigned to use or not use stereotactic navigation assistance, then tumors which were anatomically more difficult to target whose ablation was performed without navigation assistance may have required multiple more repositionings and more time and CT scans to achieve the target probe placement. Thus, for equally challenging ablations, the results from this study may underrepresent differences in the number of required probe repositionings, time to target probe placement, and total procedure time and may over-represent increased radiation dosage when using stereotactic navigation compared to without navigation assistance.

Secondly, multiple different operators performed one or more of the procedures. Different operators and assisting teams had different levels of efficiency in performing the ablation and different levels of experience. One operator may have always performed ablations using stereotactic navigation while another never used navigation assistance. The extent to which differences between the treatment groups could be accounted for simply by the variable efficiency and experience of the individual operator is unknown.

Thirdly, there was no formal standardization of the procedural operation. Once again, it is unknown how differences in the technical conduction of the procedure may have affected the overall duration of the procedure or influenced the timing between CTs. This could, for instance, lead to differences in time measurements that actually do not reflect a difference in true procedure time.

On the other hand, in some cases the stereotactic navigation system enabled ablation which otherwise would have been more complex or even impossible without image fusion. For instance, in one patient a suggested epiphyseal osteoid osteoma with typical symptoms was not detectable on CT but on MRI imaging. By using the image fusion feature of the Cas-One IR we were able to correctly fuse the pre-interventional MR-Images to the planning CT and hence target the nidus in a very difficult location, e.g. the epiphysis of the knee, without crossing or ablating the epiphyseal plate, which was located very close to the nidus.

Placing our outcomes in the context of clinical utility, these tumors are not malignant, therefore pain relief is the goal of this intervention. Completeness of resection is not predictive of longer-term outcome, as some tumors will spontaneously regress regardless of the extent of removal, and others will regrow, even if they were completely treated. Pain also does not directly correlate with tumor size. Pain is variable across individuals and a subjective outcome, and it can vary greatly simply by the location of the tumor. Similarly, larger tumors will have larger treatment zones, but that itself is not an indication of treatment success. As a result, pathology and bone defect size are not useful metrics for procedure outcome. For both groups, pain reduction, which is the most reliable clinical outcome of the procedure, was comparable for all patients. Longer-term follow-up data, if it were available, would likewise not be a good measure of the outcome of the procedure because of the intrinsic variability of the behavior of these tumors. For these reasons, we focused our study on the most objective end-points of number of needle repositionings, time to target probe placement, procedure duration, and radiation dosage.

Considering our results in the broader context of the treatment of osteoid osteomas, we report a similar safety profile to that reported in other studies. After minimally invasive ablation replaced surgical resection as the gold standard [1] of treatment for osteoid osteoma, the techniques of ablation have evolved to enhance precision

[5, 20]. The use of CT-guided therapy has significantly simplified the treatment of osteoid osteoma by enabling more precise localization of the tumor and a minimally invasive approach to the bone [5, 20, 42]. This has led to a high treatment success rate and low complication rates. The treatment outcomes of our study are consistent with the typically low complication rates of 0 to 5% [5]. Of our study patients, one experienced skin necrosis after the ablation for a complication rate of 4%.

In our study, using stereotactic navigation compared with conventional CT guidance resulted in a higher radiation dosage for the patient. This contrasts with published studies using stereotactic navigation for liver tumor ablation and various studies which reported reduced radiation using the StealthStation navigation system or robot-assisted O-arm navigation to treat osteoid osteoma [32, 33, 35, 43]. Our higher radiation exposure resulted partly from using a larger initial scan area and taking multiple control scans. With additional experience using the stereotactic navigation system, we expect fewer control scans to be required prior to attaining the desired probe positioning. The accuracy of the navigation should obviate the need for intermediate control scans. Further reduction of the dosage is anticipated by planning the puncture path more angulated to the CT plane. During an axial puncture the radiopaque metal arm of the navigation device lies in the beam path of the CT, which leads to hardening artifacts. An approach path that lies outside the CT plane would reduce these artifacts and enable fewer images to be required. Furthermore, after removal of the probe, performing the final imaging control with classical CT fluoroscopy will further reduce the radiation dosage.

In contrast to publications using stereotactic navigation for liver tumor ablation [35, 36], we found that using stereotactic navigation for ablation of osteoid osteomas did not shorten overall procedure time or reduce the total radiation dosage to the patient. However, as discussed previously, improved ease and efficiency of correct probe placement for the ablation may have been masked by the fact that our operators may have chosen to use stereotactic navigation for the more difficult procedures. Without stereotactic navigation, these procedures could have lasted considerably longer and required more probe repositionings and imaging.

Conclusion

In summary, our results comparing the use of stereotactic navigation versus conventional CT guidance for ablation of osteoid osteoma showed a higher radiation dosage to the patient when using navigation assistance without a shortening of the procedure time. The trend towards requiring one fewer probe repositioning with stereotactic navigation was not statistically conclusive with the small sample set we evaluated. However, the interpretation of these results is limited by the unknown error in the raw data measurements, the variable experience of the operators, and is confounded by the likely decision to use navigation for more difficult cases. Additional experience with the navigation system would likely enable a reduction in the radiation dosage. This highlights a learning curve necessary when starting to use the navigation system before the potential benefits of assisted navigation are realized.

Authors' contributions

C.S.: writing and data collection F.M.: data collection, writing, and analysis D.V.B.: statistical analyses, interpretation of results, manuscript writing G.N.: data collection, writing, and analysis J.H.: patient intervention procedure and data collection N.M.: patient intervention procedure, data collection, and writing.

Funding

None.

Data availability

The datasets used and/or analyzed during the current study are available from the corresponding author on reasonable request.

Declarations

Ethics approval and consent to participate

Informed consent was obtained from all of the participants in the study. The study was approved by the responsible ethics commission of Canton Bern. Project ID: 2023- 00098. The study was conducted according to the principles of the Declaration of Helsinki.

Consent for publication

No personal or identifiable details are shared within the manuscript.

Competing interests

The authors declare no competing interests.

Author details

[1]Departement Für Diagnostische, Interventionelle und Pädiatrische Radiologie, Inselspital, University Hospital Bern, University of Bern, Freiburgstrasse 10, 3010 Bern, Switzerland. [2]QuadraticMed LLC, Blegistrasse 7, 6340 Baar, Switzerland. [3]Institut für Medizinische Radiologie, Bürgerspital Solothurn, Schöngrünstrasse 42, 4500 Solothurn, Switzerland.

Received: 14 October 2024 Accepted: 2 April 2025
Published online: 29 April 2025

References

1. Jaffe HL. OSTEOID-OSTEOMA: A benign osteoblastic tumor composed of osteoid and atypical bone. Archives of Surgery. 1935;31(5):709. https://doi.org/10.1001/archsurg.1935.01180170034003.
2. Zhang Y, Rosenberg AE. Bone-Forming Tumors. Surgical Pathology Clinics. 2017;10(3):513–35. https://doi.org/10.1016/j.path.2017.04.006.
3. Boscainos PJ, Cousins GR, Kulshreshtha R, Oliver TB, Papagelopoulos PJ. Osteoid Osteoma. Orthopedics. 2013;36(10):792–800. https://doi.org/10.3928/01477447-20130920-10.
4. Shu M, Ke J. The surgical management of osteoid osteoma: A systematic review. Frontiers in Oncology. 2022;12. https://doi.org/10.3389/fonc.2022.935640.

5. Filippo MD, Russo U, Papapietro VR, Ceccarelli F, Pogliacomi F, Vaienti E, et al. Radiofrequency ablation of osteoid osteoma. Acta Biomed. 2018 Jan;89(1- S):175–185. https://doi.org/10.23750/abm.v89i1-S.7021.
6. Makley JT, Dunn MJ. Prostaglandin synthesis by osteoid osteoma. The Lancet. 1982;320(8288):42. https://doi.org/10.1016/s0140-6736(82)91174-6.
7. Kan P, Schmidt MH. Osteoid Osteoma and Osteoblastoma of the Spine. Neu- rosurgery Clinics of North America. 2008;19(1):65–70. https://doi.org/10.1016/j.nec.2007.09.003.
8. Gellman H, editor. Osteoid Osteoma. Medscape; 2023. Available from: https://emedicine.medscape.com/article/1253443-overview?form=fpf.
9. Chai JW, Hong SH, Choi JY, Koh YH, Lee JW, Choi JA, et al. Radiologic Diag- nosis of Osteoid Osteoma: From Simple to Challenging Findings. Radiographics. 2010;30(3):737–49. https://doi.org/10.1148/rg.303095120.
10. French J, Epelman M, Johnson CM, Stinson Z, Meyers AB. MR Imaging of Osteoid Osteoma: Pearls and Pitfalls. Seminars in Ultrasound, CT and MRI. 2020;41(5):488–97. https://doi.org/10.1053/j.sult.2020.05.013.
11. Liu PT, Chivers FS, Roberts CC, Schultz CJ, Beauchamp CP. Imaging of Osteoid Osteoma with Dynamic Gadolinium-enhanced MR Imaging. Radiology. 2003;227(3):691–700. https://doi.org/10.1148/radiol.2273020111.
12. Kneisl JS, Simon MA. Medical management compared with operative treatment for osteoid-osteoma. The Journal of Bone and Joint Surgery Am. 1992;74(2):179–85. https://doi.org/10.2106/00004623-199274020-00004.
13. Kitsoulis P, Mantellos G, Vlychou M. Osteoid Osteoma. Acta Orthop Belg. 2006;72(2):119–25.
14. Parmeggiani A, Martella C, Ceccarelli L, Miceli M, Spinnato P, Facchini G. Osteoid osteoma: which is the best mininvasive treatment option? European Journal of Orthopaedic Surgery and Amp. Traumatology. 2021;31(8):1611–24. https://doi.org/10.1007/s00590-021-02946-w.
15. Gangi A, Alizadeh H, Wong L, Buy X, Dietemann JL, Roy C. Osteoid Osteoma: Percutaneous Laser Ablation and Follow-up in 114 Patients. Radiology. 2007;242(1):293–301. https://doi.org/10.1148/radiol.2421041404.
16. Moser T, Giacomelli MC, Clavert JM, Buy X, Dietemann JL, Gangi A. Image-Guided Laser Ablation of Osteoid Osteoma in Pediatric Patients. Journal of Pediatric Orthopaedics. 2008;28(2):265–70. https://doi.org/10.1097/bpo.0b013e318164f472.
17. Gangi A, Dietemann JL, Gasser B, Mortazavi R, Brunner P, Mourou MY, et al. Interstitial laser photocoagulation of osteoid osteomas with use of CT guid- ance. Radiology. 1997;203(3):843–8. https://doi.org/10.1148/radiology.203.3.9169714.
18. Akhlaghpoor S, Tomasian A, Shabestari AA, Ebrahimi M, Alinaghizadeh MR. Percutaneous osteoid osteoma treatment with combination of radiofrequency and alcohol ablation. Clin Imaging. 2007;31(5):373. https://doi.org/10.1016/j.clinimag.2007.06.016.
19. Santiago E, Pauly V, Brun G, Guenoun D, Champsaur P, Corroller TL. Percutaneous cryoablation for the treatment of osteoid osteoma in the adult pop- ulation. Eur Radiol. 2018;28(6):2336–44. https://doi.org/10.1007/s00330-017-5164-6.
20. Rosenthal DI, Hornicek FJ, Wolfe MW, Jennings LC, Gebhardt MC, Mankin HJ. Percutaneous Radiofrequency Coagulation of Osteoid Osteoma Compared with Operative Treatment*. The Journal of Bone and Joint Surgery Am. 1998;80(6):815–21. https://doi.org/10.2106/00004623-199806000-00005.
21. Morassi LG, Kokkinis K, Evangelopoulos DS, Karargyris O, Vlachou I, Kalokairi- nou K, et al. Percutaneous radiofrequency ablation of spinal osteoid osteoma under CT guidance. Brit J Radiol. 2014;87(1038):20140003. https://doi.org/10.1259/bjr.20140003.
22. Igrec J, Smolle MA, Meszarics M, Godschachner TM, Steiner J, Feichtinger M, et al. A comparative study assessing the efficacy and safety of radiofrequency ablation versus surgical treatment for osteoid osteoma: retrospective analysis in a single institution. Insights into Imaging. 2024;15(1):175-85.
23. Nijland H, Gerbers JG, Bulstra SK, Overbosch J, Stevens M, Jutte PC. Evaluation of accuracy and precision of CT-guidance in Radiofrequency Ablation for osteoid osteoma in 86 patients. PLoS ONE. 2017;12(4): e0169171. https://doi.org/10.1371/journal.pone.0169171.
24. Tordjman M, Perronne L, Madelin G, Mali RD, Burke C. CT-guided radiofrequency ablation for osteoid osteomas: a systematic review. Eur Radiol. 2020;30(11):5952–63. https://doi.org/10.1007/s00330-020-06970-y.
25. Sahin C, Oc Y, Ediz N, Altınay M, Bayrak AH. The safety and the efficacy of computed tomography guided percutaneous radiofrequency ablation of osteoid osteoma. Acta Orthop Traumatol Turc. 2019;53(5):360–5. https://doi.org/10.1016/j.aott.2019.06.001.
26. Kulkarni SS, Shetty NS, Polnaya AM, Janu A, Kumar S, Puri A, et al. CT-guided radiofrequency ablation in osteoid osteoma: Result from a tertiary cancer centre in India. Indian Journal of Radiology and Imaging. 2017;27(03):318–23. https://doi.org/10.4103/ijri.ijri3017.
27. Somma F, Stoia V, D'Angelo R, Fiore F. Imaging-guided radiofrequency ablation of osteoid osteoma in typical and atypical sites: Long term follow up. PLoS ONE. 2021;16(3): e0248589. https://doi.org/10.1371/journal.pone.0248589.
28. Ati¸c R, Alemdar C, El¸ci S, Dusak A, C¸ a¸can MA, O¨ zkul E, et al. Comparative Analysis of Percutaneous Excision and Radiofrequency Ablation for Osteoid Osteoma. Medical Science Monitor. 2023;29. https://doi.org/10.12659/msm.940292.
29. Sagoo NS, Haider AS, Chen AL, Vannabouathong C, Larsen K, Sharma R, et al. Radiofrequency ablation for spinal osteoid osteoma: A systematic review of safety and treatment outcomes. Surgical Oncology. 2022;41:101747. https://doi.org/10.1016/j.suronc.2022.101747.
30. Gasbarrini A, Cappuccio M, Bandiera S, Amendola L, van Urk P, Boriani S. Osteoid Osteoma of the Mobile Spine. Spine. 2011;36(24):2089–93. https://doi.org/10.1097/brs.0b013e3181ffeb5e.
31. Rimondi E, Bianchi G, Malaguti MC, Ciminari R, Baldo AD, Mercuri M, et al. Radiofrequency thermoablation of primary non-spinal osteoid osteoma: optimization of the procedure. Eur Radiol. 2005;15(7):1393–9. https://doi.org/10.1007/s00330-004-2616-6.
32. Ankory R, Kadar A, Netzer D, Schermann H, Gortzak Y, Dadia S, et al. 3D imaging and stealth navigation instead of CT guidance for radiofrequency ablation of osteoid osteomas: a series of 52 patients. BMC Musculoskeletal Disorders. 2019;20(1). https://doi.org/10.1186/s12891-019-2963-8.
33. Wang TL, Luo YP, Zhou ZF, Liu JF, Hou XD, Jia SH, et al. O-Arm-Navigated, Robot-Assisted Versus Conventional CT Guided Radiofrequency Ablation in Treatment of Osteoid Osteoma: A Retrospective Cohort Study. Frontiers in Surgery. 2022;9. https://doi.org/10.3389/fsurg.2022.881852.
34. Cheng EY, Naranje SM. Radiofrequency Ablation of Osteoid Osteoma with Use of Intraoperative Three-Dimensional Imaging and Surgical Navigation. JBJS Essential Surgical Techniques. 2014;4(4): e22. https://doi.org/10.2106/jbjs.st.n.00094.
35. Beyer LP, Pregler B, Nießen C, Schicho A, Haimerl M, Jung EM, et al. Stereotactically-navigated percutaneous Irreversible Electroporation (IRE) compared to conventional IRE: a prospective trial. PeerJ. 2016;4: e2277. https://doi.org/10.7717/peerj.2277.
36. Schaible J, Lu¨rken L, Wiggermann P, Verloh N, Einspieler I, Zeman F, et al. Primary efficacy of percutaneous microwave ablation of malignant liver tumors: comparison of stereotactic and conventional manual guidance. Scientific Reports. 2020;10(1). https://doi.org/10.1038/s41598-020-75925-6.
37. Peterhans M, vom Berg A, Dagon B, Inderbitzin D, Baur C, Candinas D, et al. A navigation system for open liver surgery: design, workflow and first clinical applications. The International Journal of Medical Robotics and Computer Assisted Surgery. 2011;7(1):7–16. https://doi.org/10.1002/rcs.360.
38. Kruschke JK. Bayesian estimation supersedes the t test. J Exp Psychol Gen. 2013;142(2):573–603. https://doi.org/10.1037/a0029146.
39. Brooks SP. Bayesian computation: a statistical revolution. Philosophical Transactions of the Royal Society of London Series A: Mathematical, Physical and Engineering Sciences. 1813;2003(361):2681–97. https://doi.org/10.1098/rsta.2003.1263.
40. Goodman SN. Toward Evidence-Based Medical Statistics 1: The P Value Fallacy. Ann Int Med. 1999;130(12):995. https://doi.org/10.7326/0003-4819-130-12-199906150-00008.
41. on emerging SC, Risks NIH. Health effects of security scanners for passenger screening (based on X-ray technology).European Commisison, Health Systems and Products; 2012. Available from: https://ec.europa.eu/health/scientificcommittees/emerging/docs/scenihr o 036.pdf.
42. Miyazaki M, Aoki J, Miyazaki A, Nakajima T, Koyama Y, Shinozaki T, et al. Percutaneous radiofrequency ablation of osteoid osteoma using cool-tip

electrodes without the cooling system. Jpn J Radiol. 2011;29(2):138–43. https://doi.org/10.1007/s11604-010-0529-7.
43. Cheng EY, Naranje SM, Ritenour ER. Radiation Dosimetry of Intraoperative Cone-Beam Compared with Conventional CT for Radiofrequency Ablation of Osteoid Osteoma. J Bone Joint Surg. 2014;96(9):735–42. https://doi.org/10.2106/jbjs.m.00874.

Publisher's Note